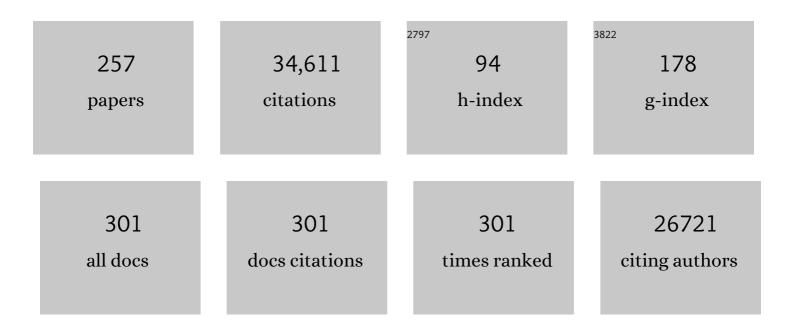
List of Publications by Year in descending order

Source: https://exaly.com/author-pdf/57936/publications.pdf Version: 2024-02-01



#	Article	IF	CITATIONS
1	Free R value: a novel statistical quantity for assessing the accuracy of crystal structures. Nature, 1992, 355, 472-475.	13.7	4,116
2	Crystal structure of a SNARE complex involved in synaptic exocytosis at 2.4 à resolution. Nature, 1998, 395, 347-353.	13.7	2,191
3	Version 1.2 of the Crystallography and NMR system. Nature Protocols, 2007, 2, 2728-2733.	5.5	1,299
4	Stochastic boundary conditions for molecular dynamics simulations of ST2 water. Chemical Physics Letters, 1984, 105, 495-500.	1.2	548
5	Determination of three-dimensional structures of proteins by simulated annealing with interproton distance restraints. Application to crambin, potato carboxypeptidase inhibitor and barley serine proteinase inhibitor 2. Protein Engineering, Design and Selection, 1988, 2, 27-38.	1.0	513
6	Polar hydrogen positions in proteins: Empirical energy placement and neutron diffraction comparison. Proteins: Structure, Function and Bioinformatics, 1988, 4, 148-156.	1.5	495
7	ATG14 promotes membrane tethering and fusion of autophagosomes to endolysosomes. Nature, 2015, 520, 563-566.	13.7	460
8	A New Generation of Crystallographic Validation Tools for the Protein Data Bank. Structure, 2011, 19, 1395-1412.	1.6	405
9	Crystallographic refinement by simulated annealing. Journal of Molecular Biology, 1988, 203, 803-816.	2.0	402
10	Torsion angle dynamics: Reduced variable conformational sampling enhances crystallographic structure refinement. Proteins: Structure, Function and Bioinformatics, 1994, 19, 277-290.	1.5	379
11	Protein Hydration Observed by X-ray Diffraction. Journal of Molecular Biology, 1994, 243, 100-115.	2.0	379
12	Checking your imagination: applications of the free R value. Structure, 1996, 4, 897-904.	1.6	379
13	Transglutaminase 2 Undergoes a Large Conformational Change upon Activation. PLoS Biology, 2007, 5, e327.	2.6	369
14	A novel evolutionarily conserved domain of cell-adhesion GPCRs mediates autoproteolysis. EMBO Journal, 2012, 31, 1364-1378.	3.5	355
15	Active site dynamics in protein molecules: A stochastic boundary molecular-dynamics approach. Biopolymers, 1985, 24, 843-865.	1.2	347
16	Complete structure of p97/valosin-containing protein reveals communication between nucleotide domains. Nature Structural and Molecular Biology, 2003, 10, 856-863.	3.6	347
17	Structural Basis of Rab Effector Specificity. Cell, 1999, 96, 363-374.	13.5	338
18	Structure of photosystem II and substrate binding at room temperature. Nature, 2016, 540, 453-457.	13.7	323

#	Article	IF	CITATIONS
19	Substrate recognition strategy for botulinum neurotoxin serotype A. Nature, 2004, 432, 925-929.	13.7	310
20	Structural Changes Are Associated with Soluble N-Ethylmaleimide-sensitive Fusion Protein Attachment Protein Receptor Complex Formation. Journal of Biological Chemistry, 1997, 272, 28036-28041.	1.6	308
21	The 1.0 Ã crystal structure of Ca2+-bound calmodulin: an analysis of disorder and implications for functionally relevant plasticity. Journal of Molecular Biology, 2000, 301, 1237-1256.	2.0	301
22	Torsion-Angle Molecular Dynamics as a New Efficient Tool for NMR Structure Calculation. Journal of Magnetic Resonance, 1997, 124, 154-164.	1.2	300
23	A dimerization motif for transmembrane α–helices. Nature Structural Biology, 1994, 1, 157-163.	9.7	294
24	Application of molecular dynamics with interproton distance restraints to three-dimensional protein structure determination. Journal of Molecular Biology, 1986, 191, 523-551.	2.0	288
25	[19] Free R value: Cross-validation in crystallography. Methods in Enzymology, 1997, 277, 366-396.	0.4	286
26	Native α-synuclein induces clustering of synaptic-vesicle mimics via binding to phospholipids and synaptobrevin-2/VAMP2. ELife, 2013, 2, e00592.	2.8	275
27	Properties of native brain α-synuclein. Nature, 2013, 498, E4-E6.	13.7	271
28	Architecture of the synaptotagmin–SNARE machinery for neuronal exocytosis. Nature, 2015, 525, 62-67.	13.7	268
29	Super-resolution biomolecular crystallography with low-resolution data. Nature, 2010, 464, 1218-1222.	13.7	267
30	Solution conformation of a heptadecapeptide comprising the DNA binding helix F of the cyclic AMP receptor protein of Escherichia coli. Journal of Molecular Biology, 1985, 186, 435-455.	2.0	256
31	Structure and function of SNARE and SNARE-interacting proteins. Quarterly Reviews of Biophysics, 2005, 38, 1.	2.4	251
32	Folding intermediates of SNARE complex assembly. Nature Structural Biology, 1999, 6, 117-123.	9.7	242
33	The three-dimensional structure of α1-purothionin in solution: combined use of nuclear magnetic resonance, distance geometry and restrained molecular dynamics. EMBO Journal, 1986, 5, 2729-2735.	3.5	241
34	Structure of the ATP-dependent oligomerization domain of N-ethylmaleimide sensitive factor complexed with ATP. Nature Structural Biology, 1998, 5, 803-811.	9.7	240
35	Identification of a Minimal Core of the Synaptic SNARE Complex Sufficient for Reversible Assembly and Disassembly. Biochemistry, 1998, 37, 10354-10362.	1.2	239
36	The primed SNARE–complexin–synaptotagmin complex for neuronal exocytosis. Nature, 2017, 548, 420-425.	13.7	229

#	Article	IF	CITATIONS
37	Interhelical hydrogen bonding drives strong interactions in membrane proteins. Nature Structural Biology, 2000, 7, 154-160.	9.7	226
38	Conformational variability in the refined structure of the chaperonin GroEL at 2.8 Ã resolution. Nature Structural and Molecular Biology, 1995, 2, 1083-1094.	3.6	219
39	Botulinum neurotoxin B recognizes its protein receptor with high affinity and specificity. Nature, 2006, 444, 1092-1095.	13.7	219
40	Structural Basis of FFAT Motif-Mediated ER Targeting. Structure, 2005, 13, 1035-1045.	1.6	218
41	Mechanistic insights into the recycling machine of the SNARE complex. Nature, 2015, 518, 61-67.	13.7	216
42	Combining Efficient Conformational Sampling with a Deformable Elastic Network Model Facilitates Structure Refinement at Low Resolution. Structure, 2007, 15, 1630-1641.	1.6	213
43	Sampling and efficiency of metric matrix distance geometry: A novel partial metrization algorithm. Journal of Biomolecular NMR, 1992, 2, 33-56.	1.6	210
44	Refinement of the influenza virus hemagglutinin by simulated annealing. Journal of Molecular Biology, 1990, 212, 737-761.	2.0	204
45	Computational searching and mutagenesis suggest a structure for the pentameric transmembrane domain of phospholamban. Nature Structural and Molecular Biology, 1995, 2, 154-162.	3.6	198
46	New applications of simulated annealing in X-ray crystallography and solution NMR. Structure, 1997, 5, 325-336.	1.6	197
47	Single-molecule FRET–derived model of the synaptotagmin 1–SNARE fusion complex. Nature Structural and Molecular Biology, 2010, 17, 318-324.	3.6	194
48	Conformational changes of the multifunction p97 AAA ATPase during its ATPase cycle. Nature Structural Biology, 2002, 9, 950-957.	9.7	189
49	Central Pore Residues Mediate the p97/VCP Activity Required for ERAD. Molecular Cell, 2006, 22, 451-462.	4.5	188
50	A ubiquitin ligase transfers preformed polyubiquitin chains from a conjugating enzyme to a substrate. Nature, 2007, 446, 333-337.	13.7	187
51	Molecular Mechanisms of Synaptic Vesicle Priming by Munc13 and Munc18. Neuron, 2017, 95, 591-607.e10.	3.8	185
52	Improved Structures of Full-Length p97, an AAA ATPase: Implications for Mechanisms of Nucleotide-Dependent Conformational Change. Structure, 2008, 16, 715-726.	1.6	181
53	Crystal Structure of the Cytosolic C2a-C2b Domains of Synaptotagmin III. Journal of Cell Biology, 1999, 147, 589-598.	2.3	179
54	Structures of Neuroligin-1 and the Neuroligin-1/Neurexin-1Î ² Complex Reveal Specific Protein-Protein and Protein-Ca2+ Interactions. Neuron, 2007, 56, 992-1003.	3.8	178

#	Article	IF	CITATIONS
55	The glycophorin A transmembrane domain dimer: Sequence-specific propensity for a right-handed supercoil of helixes. Biochemistry, 1992, 31, 12726-12732.	1.2	177
56	Algorithmic Challenges in Computational Molecular Biophysics. Journal of Computational Physics, 1999, 151, 9-48.	1.9	176
57	Crystal structure of the hCASK PDZ domain reveals the structural basis of class II PDZ domain target recognition. Nature Structural Biology, 1998, 5, 317-325.	9.7	172
58	A Structural Change Occurs upon Binding of Syntaxin to SNAP-25. Journal of Biological Chemistry, 1997, 272, 4582-4590.	1.6	167
59	Statistical analysis of predicted transmembrane α-helices. BBA - Proteins and Proteomics, 1998, 1429, 113-128.	2.1	166
60	Computational challenges for macromolecular structure determination by X-ray crystallography and solution NMRspectroscopy. Quarterly Reviews of Biophysics, 1993, 26, 49-125.	2.4	165
61	Epsin 1 Undergoes Nucleocytosolic Shuttling and Its Eps15 Interactor Nh2-Terminal Homology (Enth) Domain, Structurally Similar to Armadillo and Heat Repeats, Interacts with the Transcription Factor Promyelocytic Leukemia Zn2+ Finger Protein (Plzf). Journal of Cell Biology, 2000, 149, 537-546.	2.3	163
62	Structural and Functional Comparisons of Nucleotide Pyrophosphatase/Phosphodiesterase and Alkaline Phosphatase: Implications for Mechanism and Evolutionâ€,‡. Biochemistry, 2006, 45, 9788-9803.	1.2	158
63	Refractive index-based determination of detergent concentration and its application to the study of membrane proteins. Protein Science, 2005, 14, 2207-2211.	3.1	157
64	Nucleotide Dependent Motion and Mechanism of Action of p97/VCP. Journal of Molecular Biology, 2005, 347, 437-452.	2.0	156
65	Neurexins Physically and Functionally Interact with GABAA Receptors. Neuron, 2010, 66, 403-416.	3.8	154
66	Synaptic proteins promote calcium-triggered fast transition from point contact to full fusion. ELife, 2012, 1, e00109.	2.8	154
67	Single Molecule Observation of Liposome-Bilayer Fusion Thermally Induced by Soluble N-Ethyl Maleimide Sensitive-Factor Attachment Protein Receptors (SNAREs). Biophysical Journal, 2004, 87, 3569-3584.	0.2	153
68	Structure refinement of oligonucleotides by molecular dynamics with nuclear overhauser effect interproton distance restraints: Application to 5′ d(C-G-T-A-C-G)2. Journal of Molecular Biology, 1986, 188, 455-475.	2.0	152
69	Accessory Proteins Stabilize the Acceptor Complex for Synaptobrevin, the 1:1 Syntaxin/SNAP-25 Complex. Structure, 2008, 16, 308-320.	1.6	151
70	Improved prediction for the structure of the dimeric transmembrane domain of glycophorin A obtained through global searching. , 1996, 26, 257-261.		149
71	Structural Characterization of the Intramolecular Interaction between the SH3 and Guanylate Kinase Domains of PSD-95. Molecular Cell, 2001, 8, 1313-1325.	4.5	149
72	Rab and Arl GTPase Family Members Cooperate in the Localization of the Golgin GCC185. Cell, 2008, 132, 286-298.	13.5	147

#	Article	IF	CITATIONS
73	Mapping the conformational landscape of a dynamic enzyme by multitemperature and XFEL crystallography. ELife, 2015, 4, .	2.8	143
74	In vitro system capable of differentiating fast Ca ²⁺ -triggered content mixing from lipid exchange for mechanistic studies of neurotransmitter release. Proceedings of the National Academy of Sciences of the United States of America, 2011, 108, E304-13.	3.3	142
75	Experimentally based orientational refinement of membrane protein models: a structure for the Influenza A M2 H + channel 1 1Edited by G. von Heijne. Journal of Molecular Biology, 1999, 286, 951-962.	2.0	141
76	Ensemble molecular dynamics yields submillisecond kinetics and intermediates of membrane fusion. Proceedings of the National Academy of Sciences of the United States of America, 2006, 103, 11916-11921.	3.3	139
77	Neuronal SNAREs Do Not Trigger Fusion between Synthetic Membranes but Do Promote PEG-Mediated Membrane Fusion. Biophysical Journal, 2006, 90, 1661-1675.	0.2	134
78	Molecular Mechanisms of Fast Neurotransmitter Release. Annual Review of Biophysics, 2018, 47, 469-497.	4.5	133
79	The ENTH domain. FEBS Letters, 2002, 513, 11-18.	1.3	131
80	Role of the Â-phosphate of ATP in triggering protein folding by GroEL-GroES: function, structure and energetics. EMBO Journal, 2003, 22, 4877-4887.	3.5	130
81	Exo84 and Sec5 are competitive regulatory Sec6/8 effectors to the RalA GTPase. EMBO Journal, 2005, 24, 2064-2074.	3.5	130
82	Conformational Variability of Solution Nucelar Magnetic Resonance Structures. Journal of Molecular Biology, 1995, 250, 80-93.	2.0	123
83	Goniometer-based femtosecond crystallography with X-ray free electron lasers. Proceedings of the National Academy of Sciences of the United States of America, 2014, 111, 17122-17127.	3.3	122
84	Single-molecule studies of SNARE complex assembly reveal parallel and antiparallel configurations. Proceedings of the National Academy of Sciences of the United States of America, 2003, 100, 14800-14805.	3.3	120
85	Neuroligin-1 performs neurexin-dependent and neurexin-independent functions in synapse validation. EMBO Journal, 2009, 28, 3244-3255.	3.5	120
86	Single-wavelength anomalous diffraction phasing revisited. Acta Crystallographica Section D: Biological Crystallography, 2000, 56, 1413-1420.	2.5	116
87	Crystal Structure of the Vesicular Transport Protein Sec17. Molecular Cell, 1999, 4, 85-95.	4.5	114
88	Studying calcium-triggered vesicle fusion in a single vesicle-vesicle content and lipid-mixing system. Nature Protocols, 2013, 8, 1-16.	5.5	113
89	NSF N-Terminal Domain Crystal Structure. Molecular Cell, 1999, 4, 97-107.	4.5	112
90	Exploring the Structural Dynamics of the E.coli Chaperonin GroEL Using Translation-libration-screw Crystallographic Refinement of Intermediate States. Journal of Molecular Biology, 2004, 342, 229-245.	2.0	109

#	Article	IF	CITATIONS
91	Enabling X-ray free electron laser crystallography for challenging biological systems from a limited number of crystals. ELife, 2015, 4, .	2.8	106
92	Exploration of disorder in protein structures by X-ray restrained molecular dynamics. Proteins: Structure, Function and Bioinformatics, 1991, 10, 340-358.	1.5	105
93	Crystal Structures of a Rab Protein in its Inactive and Active Conformations. Journal of Molecular Biology, 2000, 304, 585-598.	2.0	103
94	Structural basis of the interaction between RalA and Sec5, a subunit of the sec6/8 complex. EMBO Journal, 2003, 22, 3267-3278.	3.5	103
95	[13] Crystallographic refinement by simulated annealing: Methods and applications. Methods in Enzymology, 1997, 277, 243-269.	0.4	102
96	Analysis of a Yeast SNARE Complex Reveals Remarkable Similarity to the Neuronal SNARE Complex and a Novel Function for the C Terminus of the SNAP-25 Homolog, Sec9. Journal of Biological Chemistry, 1997, 272, 16610-16617.	1.6	99
97	X-ray scattering from unilamellar lipid vesicles. Journal of Applied Crystallography, 2005, 38, 126-131.	1.9	98
98	Inhibition of Metalloprotease Botulinum Serotype A from a Pseudo-peptide Binding Mode to a Small Molecule That Is Active in Primary Neurons. Journal of Biological Chemistry, 2007, 282, 5004-5014.	1.6	98
99	Single-Molecule Studies of the Neuronal SNARE Fusion Machinery. Annual Review of Biochemistry, 2009, 78, 903-928.	5.0	98
100	De novo phasing with X-ray laser reveals mosquito larvicide BinAB structure. Nature, 2016, 539, 43-47.	13.7	98
101	Ultrahigh-resolution imaging reveals formation of neuronal SNARE/Munc18 complexes in situ. Proceedings of the National Academy of Sciences of the United States of America, 2013, 110, E2812-20.	3.3	97
102	Automated modeling of coiled coils: application to the GCN4 dimerization region. Protein Engineering, Design and Selection, 1991, 4, 649-659.	1.0	95
103	Amino-acid substitutions in a surface turn modulate protein stability. Nature Structural Biology, 1996, 3, 54-58.	9.7	95
104	Structure of a Human A-type Potassium Channel Interacting Protein DPPX, a Member of the Dipeptidyl Aminopeptidase Family. Journal of Molecular Biology, 2004, 343, 1055-1065.	2.0	92
105	Single-Molecule Studies of Synaptotagmin and Complexin Binding to the SNARE Complex. Biophysical Journal, 2005, 89, 690-702.	0.2	92
106	Botulinum Neurotoxin Heavy Chain Belt as an Intramolecular Chaperone for the Light Chain. PLoS Pathogens, 2007, 3, e113.	2.1	92
107	Receptor and substrate interactions of clostridial neurotoxins. Toxicon, 2009, 54, 550-560.	0.8	92
108	Three-dimensional molecular modeling with single molecule FRET. Journal of Structural Biology, 2011, 173, 497-505.	1.3	92

#	Article	IF	CITATIONS
109	Molecular mechanism of the synaptotagmin–SNARE interaction in Ca2+-triggered vesicle fusion. Nature Structural and Molecular Biology, 2010, 17, 325-331.	3.6	89
110	Complexin inhibits spontaneous release and synchronizes Ca2+-triggered synaptic vesicle fusion by distinct mechanisms. ELife, 2014, 3, e03756.	2.8	89
111	Advances, Interactions, and Future Developments in the CNS, Phenix, and Rosetta Structural Biology Software Systems. Annual Review of Biophysics, 2013, 42, 265-287.	4.5	88
112	A Revised Model for the Oligomeric State of the N-Ethylmaleimide-sensitive Fusion Protein, NSF. Journal of Biological Chemistry, 1998, 273, 15675-15681.	1.6	85
113	Structural insights into the molecular mechanism of Ca2+-dependent exocytosis. Current Opinion in Neurobiology, 2000, 10, 293-302.	2.0	85
114	Mechanistic insights into active site-associated polyubiquitination by the ubiquitin-conjugating enzyme Ube2g2. Proceedings of the National Academy of Sciences of the United States of America, 2009, 106, 3722-3727.	3.3	84
115	Recent developments for the efficient crystallographic refinement of macromolecular structures. Current Opinion in Structural Biology, 1998, 8, 606-611.	2.6	83
116	Transmembrane signal transduction of the \hat{I} ±llb \hat{I}^2 3 integrin. Protein Science, 2009, 11, 1800-1812.	3.1	78
117	Conformational change of syntaxin linker region induced by Munc13s initiates <scp>SNARE</scp> complex formation in synaptic exocytosis. EMBO Journal, 2017, 36, 816-829.	3.5	78
118	NSF and p97/VCP: similar at first, different at last. FEBS Letters, 2003, 555, 126-133.	1.3	77
119	Human ornithine aminotransferase complexed with L-canaline and gabaculine: structural basis for substrate recognition. Structure, 1997, 5, 1067-1075.	1.6	75
120	High Resolution Structure, Stability, and Synaptotagmin Binding of a Truncated Neuronal SNARE Complex. Journal of Biological Chemistry, 2003, 278, 8630-8636.	1.6	75
121	New insights into clostridial neurotoxin–SNARE interactions. Trends in Molecular Medicine, 2005, 11, 377-381.	3.5	75
122	Expression of C1ql3 in Discrete Neuronal Populations Controls Efferent Synapse Numbers andÂDiverse Behaviors. Neuron, 2016, 91, 1034-1051.	3.8	75
123	Successful prediction of the coiled coil geometry of the GCN4 leucine zipper domain by simulated annealing: Comparison to the X-ray structure. Proteins: Structure, Function and Bioinformatics, 1993, 15, 133-146.	1.5	73
124	A high-transparency, micro-patternable chip for X-ray diffraction analysis of microcrystals under native growth conditions. Acta Crystallographica Section D: Biological Crystallography, 2015, 71, 1987-1997.	2.5	73
125	Conformation of the synaptobrevin transmembrane domain. Proceedings of the National Academy of Sciences of the United States of America, 2006, 103, 8378-8383.	3.3	72
126	The pre-synaptic fusion machinery. Current Opinion in Structural Biology, 2019, 54, 179-188.	2.6	72

AXEL T BRUNGER

#	Article	IF	CITATIONS
127	Do NOE distances contain enough information to assess the relative populations of multi-conformer structures?. Journal of Biomolecular NMR, 1996, 7, 72-6.	1.6	71
128	Thermal Motion and Conformational Disorder in Protein Crystal Structures: Comparison of Multi onformer and Timeâ€Averaging Models. Israel Journal of Chemistry, 1994, 34, 165-175.	1.0	69
129	Solution conformations of human growth hormone releasing factor: comparison of the restrained molecular dynamics and distance geometry methods for a system without long-range distance data. Protein Engineering, Design and Selection, 1987, 1, 399-406.	1.0	68
130	Site-Directed Dichroism As a Method for Obtaining Rotational and Orientational Constraints for Oriented Polymers. Journal of the American Chemical Society, 1997, 119, 8973-8980.	6.6	68
131	Molecular Dynamics Applied to X-ray Structure Refinement. Accounts of Chemical Research, 2002, 35, 404-412.	7.6	68
132	STRUCTURAL PERSPECTIVES OF PHOSPHOLAMBAN, A HELICAL TRANSMEMBRANE PENTAMER. Annual Review of Biophysics and Biomolecular Structure, 1997, 26, 157-179.	18.3	67
133	Structural insights into the molecular mechanism of calcium-dependent vesicle–membrane fusion. Current Opinion in Structural Biology, 2001, 11, 163-173.	2.6	67
134	Considerations for the refinement of low-resolution crystal structures. Acta Crystallographica Section D: Biological Crystallography, 2006, 62, 923-932.	2.5	67
135	Structural principles of SNARE complex recognition by the AAA+ protein NSF. ELife, 2018, 7, .	2.8	67
136	Thermodynamics of protein-peptide interactions in the ribonuclease-S system studied by molecular dynamics and free energy calculations. Biochemistry, 1992, 31, 8661-8674.	1.2	66
137	C-terminal domain of mammalian complexin-1 localizes to highly curved membranes. Proceedings of the United States of America, 2016, 113, E7590-E7599.	3.3	66
138	Capture and X-ray diffraction studies of protein microcrystals in a microfluidic trap array. Acta Crystallographica Section D: Biological Crystallography, 2015, 71, 928-940.	2.5	64
139	Protein dynamics and distance determination by NOE measurements. FEBS Letters, 1988, 236, 71-76.	1.3	63
140	High-density grids for efficient data collection from multiple crystals. Acta Crystallographica Section D: Structural Biology, 2016, 72, 2-11.	1.1	62
141	Structure of Proteins Involved in Synaptic Vesicle Fusion in Neurons. Annual Review of Biophysics and Biomolecular Structure, 2001, 30, 157-171.	18.3	61
142	Structure and function of the yeast U-box-containing ubiquitin ligase Ufd2p. Proceedings of the National Academy of Sciences of the United States of America, 2007, 104, 15599-15606.	3.3	59
143	Helix packing in proteins: Prediction and energetic analysis of dimeric, trimeric, and tetrameric GCN4 coiled coil structures. Proteins: Structure, Function and Bioinformatics, 1994, 20, 105-123.	1.5	58
144	Are there dominant membrane protein families with a given number of helices?. , 1997, 28, 465-466.		58

#	Article	IF	CITATIONS
145	A Potent Peptidomimetic Inhibitor of Botulinum Neurotoxin Serotype A Has a Very Different Conformation than SNAP-25 Substrate. Structure, 2008, 16, 1588-1597.	1.6	57
146	Formation of a yeast SNARE complex is accompanied by significant structural changes. FEBS Letters, 1997, 415, 49-55.	1.3	56
147	Structures of C1q-like Proteins Reveal Unique Features among the C1q/TNF Superfamily. Structure, 2015, 23, 688-699.	1.6	56
148	Electron cryomicroscopy structure of N-ethyl maleimide sensitive factor at 11 A resolution. EMBO Journal, 2003, 22, 4365-4374.	3.5	54
149	X-ray structure determination at low resolution. Acta Crystallographica Section D: Biological Crystallography, 2009, 65, 128-133.	2.5	54
150	Simultaneous single-molecule epigenetic imaging of DNA methylation and hydroxymethylation. Proceedings of the National Academy of Sciences of the United States of America, 2016, 113, 4338-4343.	3.3	54
151	The AAA+ superfamily: a review of the structural and mechanistic principles of these molecular machines. Critical Reviews in Biochemistry and Molecular Biology, 2022, 57, 156-187.	2.3	54
152	Simulation analysis of structures on the reaction pathway of RNAse A. Journal of the American Chemical Society, 1990, 112, 3826-3831.	6.6	53
153	Conformational substrates and uncertainty in macromolecular free energy calculations. The Journal of Physical Chemistry, 1993, 97, 3409-3417.	2.9	52
154	Direct Visualization of <i>Trans</i> -Synaptic Neurexin–Neuroligin Interactions during Synapse Formation. Journal of Neuroscience, 2014, 34, 15083-15096.	1.7	51
155	Morphologies of synaptic protein membrane fusion interfaces. Proceedings of the National Academy of Sciences of the United States of America, 2017, 114, 9110-9115.	3.3	51
156	The 1.8 å crystal structure of a statically disordered 17 base-pair RNA duplex: principles of RNA crystal packing and its effect on nucleic acid structure 1 1Edited by I. Tinoco. Journal of Molecular Biology, 1999, 285, 1577-1588.	2.0	49
157	Highly specific interactions between botulinum neurotoxins and synaptic vesicle proteins. Cellular and Molecular Life Sciences, 2008, 65, 2296-2306.	2.4	49
158	Polarizable atomic multipole X-ray refinement: application to peptide crystals. Acta Crystallographica Section D: Biological Crystallography, 2009, 65, 952-965.	2.5	49
159	Complexin-1 Enhances the On-Rate of Vesicle Docking via Simultaneous SNARE and Membrane Interactions. Journal of the American Chemical Society, 2013, 135, 15274-15277.	6.6	49
160	Mutational Analysis of Synaptobrevin Transmembrane Domain Oligomerizationâ€. Biochemistry, 2002, 41, 15861-15866.	1.2	47
161	The Structure of the Yeast Plasma Membrane SNARE Complex Reveals Destabilizing Water-filled Cavities. Journal of Biological Chemistry, 2008, 283, 1113-1119.	1.6	47
162	Towards reconstitution of membrane fusion mediated by SNAREs and other synaptic proteins. Critical Reviews in Biochemistry and Molecular Biology, 2015, 50, 231-241.	2.3	47

#	Article	IF	CITATIONS
163	Recent Advances in Deciphering the Structure and Molecular Mechanism of the AAA+ ATPase N-Ethylmaleimide-Sensitive Factor (NSF). Journal of Molecular Biology, 2016, 428, 1912-1926.	2.0	47
164	Dramatic Structural and Thermodynamic Consequences of Repacking a Protein's Hydrophobic Core. Structure, 2000, 8, 1319-1328.	1.6	46
165	2.3 à Crystal Structure of Tetanus Neurotoxin Light Chainâ€,‡. Biochemistry, 2005, 44, 7450-7457.	1.2	46
166	Structural and Biochemical Studies of Botulinum Neurotoxin Serotype C1 Light Chain Protease: Implications for Dual Substrate Specificity [,] . Biochemistry, 2007, 46, 10685-10693.	1.2	46
167	Ca2+-Triggered Synaptic Vesicle Fusion Initiated by Release of Inhibition. Trends in Cell Biology, 2018, 28, 631-645.	3.6	46
168	A comparison of the restrained molecular dynamics and distance geometry methods for determining three-dimensional structures of proteins on the basis of interproton distances. FEBS Letters, 1987, 213, 269-277.	1.3	44
169	Crystallographic evidence for deviating C3b structure. Nature, 2007, 448, E1-E2.	13.7	44
170	N-terminal domain of complexin independently activates calcium-triggered fusion. Proceedings of the National Academy of Sciences of the United States of America, 2016, 113, E4698-E4707.	3.3	44
171	The protein-folding problem: Not yet solved. Science, 2022, 375, 507-507.	6.0	43
172	Processive ATP-driven Substrate Disassembly by the N-Ethylmaleimide-sensitive Factor (NSF) Molecular Machine. Journal of Biological Chemistry, 2013, 288, 23436-23445.	1.6	40
173	Phosphorylation of residues inside the <scp>SNARE</scp> complex suppresses secretory vesicle fusion. EMBO Journal, 2016, 35, 1810-1821.	3.5	40
174	Inhibition of calcium-triggered secretion by hydrocarbon-stapled peptides. Nature, 2022, 603, 949-956.	13.7	39
175	Influence of internal dynamics on accuracy of protein NMR structures: derivation of realistic model distance data from a long molecular dynamics trajectory 1 1Edited by G. Von Heijne. Journal of Molecular Biology, 1999, 285, 727-740.	2.0	38
176	Determination of the backbone conformation of secretin by restrained molecular dynamics on the basis of interproton distance data. FEBS Journal, 1988, 171, 479-484.	0.2	37
177	The Longin SNARE VAMP7/TI-VAMP Adopts a Closed Conformation. Journal of Biological Chemistry, 2010, 285, 17965-17973.	1.6	37
178	Improving the Accuracy of Macromolecular Structure Refinement at 7ÂÃ Resolution. Structure, 2012, 20, 957-966.	1.6	37
179	Improved crystallographic models through iterated local density-guided model deformation and reciprocal-space refinement. Acta Crystallographica Section D: Biological Crystallography, 2012, 68, 861-870.	2.5	37
180	Model morphing and sequence assignment after molecular replacement. Acta Crystallographica Section D: Biological Crystallography, 2013, 69, 2244-2250.	2.5	37

#	Article	IF	CITATIONS
181	Reintroducing Electrostatics into Macromolecular Crystallographic Refinement: Application to Neutron Crystallography and DNA Hydration. Structure, 2011, 19, 523-533.	1.6	36
182	Complexin induces a conformational change at the membrane-proximal C-terminal end of the SNARE complex. ELife, 2016, 5, .	2.8	36
183	Automatic Solution of Heavy-Atom Substructures. Methods in Enzymology, 2003, 374, 37-83.	0.4	34
184	Disassembly of All SNARE Complexes by N-Ethylmaleimide-sensitive Factor (NSF) Is Initiated by a Conserved 1:1 Interaction between α-Soluble NSF Attachment Protein (SNAP) and SNARE Complex*. Journal of Biological Chemistry, 2013, 288, 24984-24991.	1.6	34
185	NSF-mediated disassembly of on- and off-pathway SNARE complexes and inhibition by complexin. ELife, 2018, 7, .	2.8	34
186	Continuous fluorescence microphotolysis to observe lateral diffusion in membranes. Theoretical methods and applications. Journal of Chemical Physics, 1985, 82, 2147-2160.	1.2	33
187	Non-Boltzmann thermodynamic integration (NBTI) for macromolecular systems: Relative free energy of binding of trypsin to benzamidine and benzylamine. , 1999, 37, 641-653.		33
188	[32] Patterson correlation searches and refinement. Methods in Enzymology, 1997, 276, 558-580.	0.4	32
189	Post-Translational Modifications and Lipid Binding Profile of Insect Cell-Expressed Full-Length Mammalian Synaptotagmin 1. Biochemistry, 2011, 50, 9998-10012.	1.2	31
190	Role of Aberrant Spontaneous Neurotransmission in SNAP25-Associated Encephalopathies. Neuron, 2021, 109, 59-72.e5.	3.8	31
191	Prefused lysosomes cluster on autophagosomes regulated by VAMP8. Cell Death and Disease, 2021, 12, 939.	2.7	31
192	Extending the limits of molecular replacement through combined simulated annealing and maximum-likelihood refinement. Acta Crystallographica Section D: Biological Crystallography, 1999, 55, 181-190.	2.5	30
193	A highly automated heavy-atom search procedure for macromolecular structures. Acta Crystallographica Section D: Biological Crystallography, 1999, 55, 1568-1577.	2.5	30
194	Domain flexibility in the 1.75â€Ã resolution structure of Pb2+-calmodulin. Acta Crystallographica Section D: Biological Crystallography, 2003, 59, 1782-1792.	2.5	30
195	Classical and Quantum Simulations of Tryptophan in Solution. Journal of Physical Chemistry A, 1997, 101, 1935-1945.	1.1	29
196	Polarizable Atomic Multipole X-Ray Refinement: Hydration Geometry and Application to Macromolecules. Biophysical Journal, 2010, 98, 2984-2992.	0.2	29
197	Beltless Translocation Domain of Botulinum Neurotoxin A Embodies a Minimum Ion-conductive Channel. Journal of Biological Chemistry, 2012, 287, 1657-1661.	1.6	29
198	Deformable elastic network refinement for low-resolution macromolecular crystallography. Acta Crystallographica Section D: Biological Crystallography, 2014, 70, 2241-2255.	2.5	29

#	Article	IF	CITATIONS
199	2·9Ãresolution structure of an anti-dinitrophenyl-spin-label monoclonal antibody Fab fragment with bound hapten. Journal of Molecular Biology, 1991, 221, 239-256.	2.0	28
200	Phase Improvement by Multi-Start Simulated Annealing Refinement and Structure-Factor Averaging. Journal of Applied Crystallography, 1998, 31, 798-805.	1.9	28
201	<i>Data Exploration Toolkit</i> for serial diffraction experiments. Acta Crystallographica Section D: Biological Crystallography, 2015, 71, 352-356.	2.5	28
202	Advances in X-ray free electron laser (XFEL) diffraction data processing applied to the crystal structure of the synaptotagmin-1 / SNARE complex. ELife, 2016, 5, .	2.8	28
203	Application of DEN refinement and automated model building to a difficult case of molecular-replacement phasing: the structure of a putative succinyl-diaminopimelate desuccinylase from <i>Corynebacterium glutamicum</i> . Acta Crystallographica Section D: Biological Crystallography. 2012. 68. 391-403.	2.5	26
204	Sampling Properties of Simulated Annealing and Distance Geometry. , 1991, , 451-455.		26
205	Deorphanizing FAM19A proteins as pan-neurexin ligands with an unusual biosynthetic binding mechanism. Journal of Cell Biology, 2020, 219, .	2.3	26
206	Crystallographic phasing and refinement of macromolecules. Current Opinion in Structural Biology, 1991, 1, 1016-1022.	2.6	25
207	Helicity, membrane incorporation, orientation and thermal stability of the large conductance mechanosensitive ion channel from E. coli. Biochimica Et Biophysica Acta - Biomembranes, 1998, 1369, 131-140.	1.4	25
208	Annealing in crystallography: a powerful optimization tool. Progress in Biophysics and Molecular Biology, 1999, 72, 135-155.	1.4	25
209	Crystal Structure of a Hyperactive Escherichia coli Glycerol Kinase Mutant Gly230 → Asp Obtained Using Microfluidic Crystallization Devices,. Biochemistry, 2007, 46, 5722-5731.	1.2	25
210	Structural conservation among variants of the SARS-CoV-2 spike postfusion bundle. Proceedings of the United States of America, 2022, 119, e2119467119.	3.3	25
211	Studying proteinâ€reconstituted proteoliposome fusion with content indicators in vitro. BioEssays, 2013, 35, 658-665.	1.2	24
212	A Network Thermodynamic Investigation of Stationary and Non-Stationary Proton Transport Through Proteins. Zeitschrift Fur Physikalische Chemie, 1983, 136, 1-63.	1.4	23
213	Synaptic vesicle fusion: today and beyond. Nature Structural and Molecular Biology, 2019, 26, 663-668.	3.6	23
214	lterative Structure-Based Peptide-Like Inhibitor Design against the Botulinum Neurotoxin Serotype A. PLoS ONE, 2010, 5, e11378.	1.1	22
215	Conformational dynamics of auto-inhibition in the ER calcium sensor STIM1. ELife, 2021, 10, .	2.8	22
216	Proline <i>cisâ€trans</i> isomerization in staphylococcal nuclease: Multiâ€substate free energy perturbation calculations. Protein Science, 1995, 4, 636-654.	3.1	21

#	Article	IF	CITATIONS
217	Sec17/Sec18 can support membrane fusion without help from completion of SNARE zippering. ELife, 2021, 10, .	2.8	20
218	Storing diffraction data. Nature, 1996, 383, 18-19.	13.7	19
219	A smooth and differentiable bulk-solvent model for macromolecular diffraction. Acta Crystallographica Section D: Biological Crystallography, 2010, 66, 1024-1031.	2.5	19
220	Structures of neurexophilin–neurexin complexes reveal a regulatory mechanism of alternative splicing. EMBO Journal, 2019, 38, e101603.	3.5	19
221	A grid-enabled web service for low-resolution crystal structure refinement. Acta Crystallographica Section D: Biological Crystallography, 2012, 68, 261-267.	2.5	17
222	Munc18a Does Not Alter Fusion Rates Mediated by Neuronal SNAREs, Synaptotagmin, and Complexin. Journal of Biological Chemistry, 2015, 290, 10518-10534.	1.6	17
223	IOTA: integration optimization, triage and analysis tool for the processing of XFEL diffraction images. Journal of Applied Crystallography, 2016, 49, 1057-1064.	1.9	17
224	Tools to Assist Determination and Validation of Carbohydrate 3D Structure Data. Methods in Molecular Biology, 2015, 1273, 229-240.	0.4	16
225	Low-Resolution Crystallography Is Coming of Age. Structure, 2005, 13, 171-172.	1.6	15
226	Ab initiomolecular-replacement phasing for symmetric helical membrane proteins. Acta Crystallographica Section D: Biological Crystallography, 2007, 63, 188-196.	2.5	14
227	Automated crystallographic ligand building using the medial axis transform of an electron-density isosurface. Acta Crystallographica Section D: Biological Crystallography, 2005, 61, 1354-1363.	2.5	13
228	Recent Developments for Crystallographic Refinement of Macromolecules. , 1996, 56, 245-266.		12
229	Overcoming barriers in macromolecular simulations: non-Boltzmann thermodynamic integration. Theoretical Chemistry Accounts, 1998, 98, 171-181.	0.5	11
230	A hybrid machine-learning approach for segmentation of protein localization data. Bioinformatics, 2005, 21, 3778-3786.	1.8	11
231	Models for the Transmembrane Region of the Phospholamban Pentamer: Which Is Correct? a. Annals of the New York Academy of Sciences, 1998, 853, 178-185.	1.8	9
232	Structure Determination of Antibodies and Antibody-Antigen Complexes by Molecular Replacement. ImmunoMethods, 1993, 3, 180-190.	0.8	8
233	NMR structure calculation methods for large proteins Application of torsion angle dynamics and distance geometry/simulated annealing to the 269-residue protein serine protease PB92. Molecular Physics, 1998, 95, 1099-1112.	0.8	8
234	Molecular Characterization of AMPA-Receptor-Containing Vesicles. Frontiers in Molecular Neuroscience, 2021, 14, 754631.	1.4	8

#	Article	IF	CITATIONS
235	Free energy calculations in globular proteins: Methods to reduce errors. Journal of Computational Chemistry, 1998, 19, 1229-1240.	1.5	6
236	Quantitative Imaging of Lymphocyte Membrane Protein Reorganization and Signaling. Biophysical Journal, 2005, 88, 579-589.	0.2	6
237	Atomic resolution experimental phase information reveals extensive disorder and bound 2-methyl-2,4-pentanediol in Ca ²⁺ -calmodulin. Acta Crystallographica Section D: Structural Biology, 2016, 72, 83-92.	1.1	6
238	Improved prediction for the structure of the dimeric transmembrane domain of glycophorin A obtained through global searching. Proteins: Structure, Function and Bioinformatics, 1996, 26, 257-261.	1.5	6
239	Screening of Hydrocarbon-Stapled Peptides for Inhibition of Calcium-Triggered Exocytosis. Frontiers in Pharmacology, 0, 13, .	1.6	6
240	Warren L. DeLano 21 June 1972–3 November 2009. Nature Structural and Molecular Biology, 2009, 16, 1202-1203.	3.6	4
241	A feature-guided, focused 3D signal permutation method for subtomogram averaging. Journal of Structural Biology, 2022, 214, 107851.	1.3	4
242	Gently does it for submicron crystals. ELife, 2013, 2, e01662.	2.8	3
243	Refinement of Three-dimensional Structures of Proteins and Nucleic Acids. , 1991, , 137-178.		2
244	New Applications of Simulated Annealing in Crystallographic Refinement. , 1998, , 143-157.		2
245	Interactions Between Botulinum Neurotoxins and Synaptic Vesicle Proteins. , 2009, , 41-52.e2.		1
246	Deformable modeling for improved calculation of molecular velocities from single-particle tracking. , 2005, , 208-11.		0
247	Computational Aspects of High-Throughput Crystallographic Macromolecular Structure Determination. Methods of Biochemical Analysis, 2005, 44, 75-87.	0.2	Ο
248	Macromolecular Models by Single Molecule FRET. NATO Science for Peace and Security Series B: Physics and Biophysics, 2012, , 1-19.	0.2	0
249	New Insights into the Molecular Mechanism of Calcium-Triggered Synaptic Vesicle Fusion. Biophysical Journal, 2014, 106, 11a.	0.2	Ο
250	Molecular Mechanism of the Synaptotagmin-SNARE Complex that is Essential for Synchronous Synaptic Neurotransmitter Release. Biophysical Journal, 2016, 110, 318a.	0.2	0
251	Mechanistic Insights into NSF Mediated SNARE Complex Disassembly. Biophysical Journal, 2017, 112, 31a.	0.2	0
252	Inhibition of Airway Epithelial Snare/Synaptotagmin Mediated Membrane Fusion by Hydrocarbon-Stapled Peptides. Biophysical Journal, 2020, 118, 399a-400a.	0.2	0

#	Article	IF	CITATIONS
253	Conformational Dynamics of SNARE Proteins during NSFâ€Mediated Disassembly. FASEB Journal, 2021, 35,	0.2	0
254	The Structure of Nucleotide Pyrophosphatase/ Phosphodiesterase and Implications for Enzyme Evolution in the Alkaline Phosphatase Superfamily. FASEB Journal, 2006, 20, A477.	0.2	0
255	NMR Studies of the 269 Residue Serine Protease PB92 from Bacillus Alcalophilus. , 1999, , 227-246.		0
256	Resolving indexing ambiguities in X-ray free-electron laser diffraction patterns. Acta Crystallographica Section D: Structural Biology, 2019, 75, 234-241.	1.1	0
257	Processing simultaneously collected MAD data from two closely spaced (90â€eV) wavelengths measured at an X-ray free-electron laser. Acta Crystallographica Section A: Foundations and Advances, 2019, 75, a242-a242.	0.0	0